Computer Methods and Programs in Biomedicine 187 (2020) 105325

Contents lists available at ScienceDirect

Computer Methods and Programs in Biomedicine

journal homepage: www.elsevier.com/locate/cmpb

A flexible analytic wavelet transform based approach for motor-imagery tasks classification in BCI applications

Shalu Chaudhary[a], Sachin Taran[a], Varun Bajaj[a,*], Siuly Siuly[b]

[a] Discipline of Electronics and Communication Engineering, PDPM Indian Institute of Information Technology, Design and Manufacturing, Jabalpur 452005, India

[b] Institute for Sustainable Industries & Liveable Cities, Victoria University, Melbourne, Australia

ARTICLE INFO

Article history:
Received 9 April 2019
Revised 16 December 2019
Accepted 8 January 2020

Keywords:
Electroencephalogram(EEG) signal
Brain-Computer interface system
Motor imagery
Flexible analytic wavelet transform
Ensemble methods

ABSTRACT

Background and Objective: Motor Imagery (MI) based Brain-Computer-Interface (BCI) is a rising support system that can assist disabled people to communicate with the real world, without any external help. It serves as an alternative communication channel between the user and computer. Electroencephalogram (EEG) recordings prove to be an appropriate choice for imaging MI tasks in a BCI system as it provides a non-invasive way for completing the task. The reliability of a BCI system confides on the efficiency of the assessment of different MI tasks.

Methods: The present work proposes a new approach for the classification of distinct MI tasks based on EEG signals using the flexible analytic wavelet transform (FAWT) technique. The FAWT decomposes the EEG signal into sub-bands and temporal moment-based features are extracted from the sub-bands. Feature normalization is applied to minimize the bias nature of classifier. The FAWT-based features are utilized as inputs to multiple classifiers. Ensemble learning method based Subspace k-Nearest Neighbour (kNN) classifier is established as the best and robust classifier for the distinction of the right hand (RH) and right foot (RF) MI tasks.

Results: The sub-band (SB) wise features are tested on multiple classifiers and best performance parameters are obtained using the ensemble method based subspace kNN classifier. The best results of parameters are obtained for fourth SB as accuracy 99.33%, sensitivity 99%, specificity 99.6%, F1-Score 0.9925, and kappa value 0.9865. The other sub-bands are also attained significant results using subspace KNN classifier.

Conclusions: The proposed work explores the utility of FAWT based features for the classification of RH and RF MI tasks EEG signals. The suggested work highlights the effectiveness of multiple classifiers for classification MI-tasks. The proposed method shows better performance in comparison to state-of-arts methods. Thus, the potential to implement a BCI system for controlling wheelchairs, robotic arms, etc.

1. Introduction

Brain computer interface (BCI) is a new frontier assistive communication technology to establish a direct relationship between a computer and the human brain. It is basically a system where a series of thoughts originated from the brain are interpreted as commands to control an external device. Thus it gives the power to regulate external equipment or an appliance by forming a direct interface with the user's brain [1]. Motor Imagery (MI)-based BCI stands out among other BCI systems due to its advantage of independence of any body movement or external stimulation [2]. The MI-tasks can be considered as perceiving a motor act, for example, movement of foot, tongue, and hands beyond any physical motor activity. An individual act is generally considered as a class [3]. This enables the user to carry out a task just by imagining it. It acts as an alternate communication channel for the human by translating neural responses into a computer command. Hence, it creates a direct pathway that can assist disabled people to communicate, to control and drive external equipment independently, using just their brain activity. The biggest motivation behind the present work is to provide an advanced communication pathway for those with impairments such as spinal cord injury, traumatic brain injury and amyotrophic lateral sclerosis.

* Corresponding author.
E-mail addresses: shaluchaudhary@iiitdmj.ac.in (S. Chaudhary), sachin.taran@iiitdmj.ac.in (S. Taran), varunb@iiitdmj.ac.in (V. Bajaj), siuly.siuly@vu.edu.au (S. Siuly).

https://doi.org/10.1016/j.cmpb.2020.105325
0169-2607/

Numerous techniques have been applied for evaluation of motor imagery tasks in a BCI system but Electroencephalogram (EEG) based methods have proven to be the best. They are befitting because EEG signals provide a non-invasive way of estimating MI tasks with good time resolution [4]. Other advantages include exceptional temporal resolution, low setup costs usability, portability and inexpensiveness [4,5]. Therefore, MI-based BCI systems work by exploiting the activity patterns from EEG signals. It has shown satisfactory interrelation with physiology and mental activity of the human brain which helps in recognition of epileptic seizure and sleep stages [6]. In the literature, multiple signal processing techniques have been tested for BCI related EEG analysis with time, frequency and time-frequency domain evaluation being the major tools employed for the same purpose. Diverse methods have been employed in the EEG signal processing before going to the discrimination of MI tasks. Recently, machine learning approaches have proven to be an apt choice for the recognition of different MI activities, where feature extraction is carried out using a particular signal processing approach, succeeded by classification [7].

In [8], feature extraction process utilizing common spatial pattern (CSP) has been extensively explored for MI tasks classification. An algorithm namely temporally constrained sparse group spatial patterns (TSGSP) employing CSP and was Linear SVM was introduced in [9]. In [10], wavelet coherence (WC) was used to distinguish two MI tasks, i.e., right hand (RH) and right foot (RF) applying CSP (with and without regularization) as a pre-processing technique. CSP and chaotic particle swarm optimization (CPSO) TWSVM scheme were presented for the distinction of MI EEG signals with TWSVM classifier in [11]. Deep learning approach was adopted for classifying MI-BCI signals where feature extraction is based on CSP and deep neural network classifies the signals [12]. The presented work in [13] combines CSP algorithm along with particle swarm optimization (PSO) least square SVM classifier for recognition of patterns in MI. In [14], the aggregated regularized CSP (RCSP) was applied to categorize MI tasks based on EEG signals. Suk and Lee [15] reported a Bayesian framework considering ERD/ERS for classification purpose. Several methods have been given using LS-SVM algorithm such as a cross-correlation (CC) based technique for improving classification performance of two class MI signals [16]. Similarly, in [17], a clustering approach based LS-SVM is reported for the classification. Siuly et al. [18] introduced an optimum allocation sampling (OAS) based scheme for extracting representative features from MI-based EEG signals. Those were used as input to the naive-Bayes (NB) algorithm. In [19], wavelet packet decomposition provided best results with KNN classifier and higher order statistical features. In [20], a bispectrum based feature extraction method was proposed for identifying right and left MI. They employed SVM, LDA, and NN classifiers on the given features for better accuracy. Another work is presented in literature where extraction of features is done from the phase space of EEG signals for classifying left/right hand MI using LDA classifier [21]. Another OAS based approach is developed where LS-SVM is applied for discriminating the MI activities [22].

Several other methods have also shown their utility for MI tasks recognition and classification such as cross-correlation technique has been implemented using NB Classifier. This work implements one versus the rest approach for multiclass classification [23]. Phase space features (PSF) derived by the amplitude frequency analysis (AFA) system in the state space of EEG signals, combined with LDA classifiers is given for separation of left and right hand EEG signals [24]. Subject-specific motor imagery based EEG patterns is adaptively extracted and classified in the space-time-frequency plane using linear SVM as classifier [25]. Alam and Samanta [26] used EMD method for characterizing MI activities. Another work devises tunable Q-wavelet transform (TQWT) as feature extractor and LS-SVM as the classifier for the categorization of MI activities [27]. Identification of MI tasks was presented using CC-LR algorithm which was tested on various algorithms such as clustering technique (CT) based LS-SVM [28]. A technique using analytic intrinsic mode functions based features and LS-SVM as the classifier is given for categorization of EEG signals of different MI tasks [29]. MI activity classification has also been proposed using discrete wavelet transform (DWT) and cross-correlated signal features [30].

An LDB approach has been proposed in the literature that uses CSP as transform function and LDA is used for classification purpose [31]. In [32], multi-class classification is done using Fisher discriminant analysis-type F-score and few Laplacian EEG channels. The utility of kernel-constructed ELM classifier is also explored to distinguish signals of MI tasks [33]. In [34], a brain-machine interface (BMI) system is devised to regulate robotic arm, employing SVM classifier for identifying different MI tasks. Recently, flexible analytic wavelet transform (FAWT) has gained immense popularity and has been extensively applied for various applications. It has been used in the detection of coronary artery disease (CAD) using heart rate variability (HRV) signals. It decomposes these HRV signals into sub-band signals [35]. Another technique uses analytic time-frequency flexible wavelet transform (ATFFWT) for detection of J wave [36]. Damage detection in rotating machinery is done using flexible analytic wavelet transform by extracting weak fault signature [37]. Focal EEG signals are automatically detected using FAWT [38]. Automatic detection of epileptic seizures along with fractal dimension (FD) has been explored [39]. FAWT based features have been explored for classification of emotions using a single EEG channel [40]. It has proven to be a reliable and versatile approach due to its desirable properties that overcome the shortcomings of other wavelet transform methods. The major objective of this study is to develop a reliable classification system for identifying distinct MI tasks, such as right hand, left hand, foot, and tongue movement from non-stationary and subject-specific EEG signals. In addition, we investigate whether a flexible analytic wavelet transform (FAWT) technique is an appropriate method for feature extraction in an EEG-based MI data. The effectiveness of these systems relies on their accuracy and efficiency. It could have a large influence on the quality of life of its beneficiaries.

In the present context, the utility of FAWT is analyzed for the classification of RH and RF MI tasks based on EEG signals. It is used to extract features from the brain signals (e.g. EEG signals) by decomposing the signals into sub-bands (SBs). Using this recent time estimation method, the nonstationary EEG signals are dissolved into band-limited SBs. The time domain measures of these resulting SBs, namely temporal moment (TM3, TM4, and TM5) are contemplated as features for EEG signals. The MI tasks differentiation competency of these extracted features is further estimated by Kruskal Wallis (KW) statistical test. The selected features are tested on multiple classifiers. Multiple classifier systems are employed to evaluate the best classification performance. The remaining paper is organized as follows: Section 2 depicts our dataset used, elucidates our signal decomposition method FAWT, followed by feature extraction, selection, and normalization scheme. The classifier used is presented next. The experimental results are expounded in Section 3 followed by detailed discussion in Section 4. Lastly, Section 5 concludes this paper.

2. Methodology

The schematic representation of the FAWT based approach for classification of motor imagery activity based EEG signals is illustrated in Fig. 1. EEG signals of diverse brain activity produced by the user's brain are recognized by a system and then transformed into commands. These commands are further used by the user as feedback to communicate with external devices. In the proposed

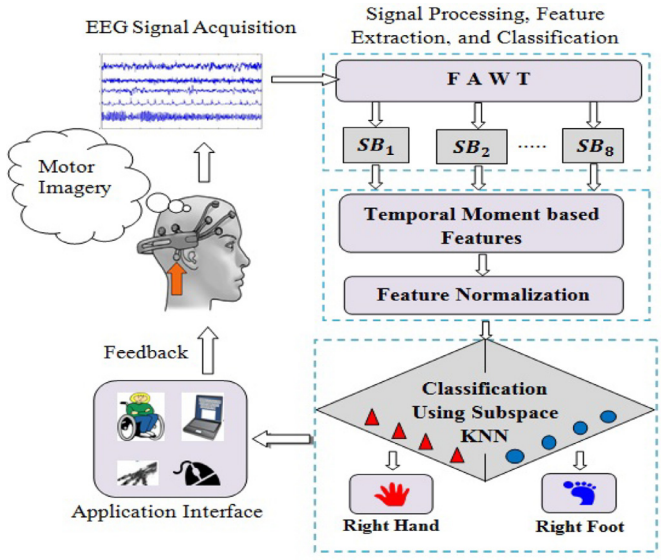

Fig. 1. Proposed approach for the classification of MI tasks.

scheme, at first, we employ FAWT method for decomposition of EEG signal into sub-bands. Then, the extracted and selected features are used as input to multiple classifier systems to assess the performance of the presented approach.

2.1. Dataset

The proposed work employs dataset IV-A of BCI competition III [41]. EEG signals of various MI tasks by locating them at the sites of the extended international 10/20 system. The subject had to perform three motor imageries: (F) right foot, (R) right hand, (L) left hand, and thus in each capturing session of this dataset, visual signs were shown to the subject for 3.5 s before EEG recording implying the same. The target sign demonstration was delayed by random interval durations allowing the subject to relax. Only the EEG data set correlative to RH and RF motor imageries of five subjects "*aa*", "*al*", "*av*", "*aw*" and "*ay*" is accessible to the public. Initially, the EEG signals were recorded at 1000 Hz but these trials are perhaps infected with artifacts like eye movements and muscle activation, which are recognized and eliminated by surface EOG and EMG signals recordings. Subsequently, down-sampling to 100 Hz followed by band-pass filtering was done in order to minimize the remaining artifacts existing in recorded EEG signals [41].

2.2. Flexible analytic wavelet transform (FAWT)

Wavelet transform (WT) is counted as one of the robust mathematical tools for processing non-stationary signals. Though WT and its various improved methods still play a vital role in the signal processing field, they have their own limitations such as CWT has confined computational efficiency whereas DWT endures shift variance and low resolution at high-frequency sub-bands [35].

2.2.1. Parameters of FAWT

The parameters a_1, a_2, a_3, a_4 and β provide flexibility to control dilation factor d, redundancy factor R and quality-factor (Q-factor) Q, where a_1 and a_2 are up and down sampling parameters of low pass filter respectively and similarly, a_3 and a_4 are up and down-sampling parameters for high pass filter respectively, whereas β is the parameter controlling Q [42].

The ratio of the center frequency and the bandwidth is represented as Q factor whereas the ratio of the output samples to the input samples corresponds to redundancy. Dilation factor regulates the size of the wavelet. These are defined as follows [42]:

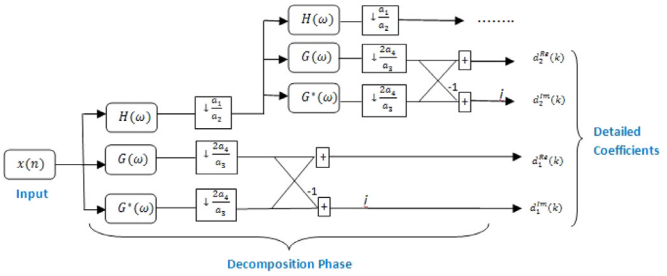

Fig. 2. FAWT decomposition algorithm.

$$Q \approx \frac{2-\beta}{\beta}, \quad d \approx \frac{a_1}{a_2}, \tag{1}$$

$$\beta \leq 1, \tag{2}$$

$$R \approx \left(\frac{a_3}{a_4}\right)\frac{1}{1-d}, \tag{3}$$

$$R > \frac{\beta}{1-d} \tag{4}$$

It can be seen that the parameters are dependent on each other.

2.2.2. Filter banks of FAWT

FAWT is accomplished by iterative filterbank (IFB) that comprises one low pass (LP) channel and two high pass (HP) channels making it suitable for long signals. One of the HP channels evaluates positive frequencies and the other conform to negative frequencies. Such dissolution of positive and negative frequency approves to exploit random sampling rates in HP channels and outputs Hilbert transform pairs of wavelet bases. FAWT can achieve decomposition up till Jth level using IFB [42]. The decomposition algorithm is presented in Fig. 2.

The frequency response of LP filter or scaling function $H(\omega)$ is given by following equation [42]:

$$H(\omega) = \begin{cases} \sqrt{a_1 a_2}, & |\omega| < \omega_p \\ \sqrt{a_1 a_2}\,\theta\left(\frac{\omega-\omega_p}{\omega_s-\omega_p}\right), & \omega_p \leq |\omega| \leq \omega_s \\ \sqrt{a_1 a_2}\,\theta\left(\frac{\pi-\omega+\omega_p}{\omega_s-\omega_p}\right), & -\omega_s \leq |\omega| \leq -\omega_p \\ 0, & |\omega| \geq \omega_s \end{cases} \tag{5}$$

ω_s and ω_p symbolize the stop band and pass band frequencies of LP filter [43] given by,

$$\omega_p = \frac{(1-\beta)\pi}{a_1} + \frac{\epsilon}{a_1}, \qquad \omega_s = \frac{\pi}{a_2}, \tag{6}$$

Similarly, HP filter or analytic wavelet function $G(\omega)$ is defined mathematically as [43]:

$$G(\omega) = \begin{cases} \sqrt{2a_3 a_4}\,\theta\left(\frac{\pi-\omega-\omega_0}{\omega_1-\omega_0}\right), & \omega_0 \leq \omega < \omega_1 \\ \sqrt{2a_3 a_4}, & \omega_1 \leq \omega < \omega_2 \\ \sqrt{2a_3 a_4}\,\theta\left(\frac{\omega-\omega_2}{\omega_3-\omega_2}\right), & \omega_2 \leq \omega \leq \omega_3 \\ 0, & \omega \in [0,\omega_0)\bigcup(\omega_3, 2\pi) \end{cases} \tag{7}$$

The frequency response of the above filters is represented in Fig. 3.

Rest of the parameters are given as follows [42]:

$$\omega_0 = \frac{(1-\beta)\pi}{a_3}, \qquad \omega_1 = \frac{a_1\pi}{a_2 a_3}, \tag{8}$$

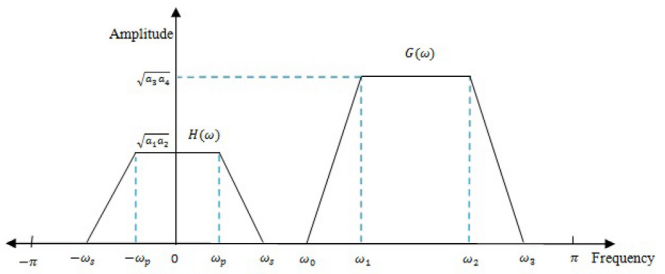

Fig. 3. Frequency response of FAWT filters.

$$\omega_2 = \frac{\pi - \epsilon}{a_3}, \qquad \omega_2 = \frac{\pi + \epsilon}{a_3}, \tag{9}$$

$$\epsilon \leq \left(\frac{a_1 - a_2 + a_2\beta}{a_1 + a_2}\right)\pi, \tag{10}$$

Transition band [42] is given as:

$$\theta(\omega) = \frac{[1 + \cos(\omega)]\sqrt{2 - \cos(\omega)}}{2}, \qquad \omega \in [0, \pi] \tag{11}$$

Daubechies' orthonormal wavelet filters using two vanishing moments is employed for formulating this transform. The absolute reformation filter bank can be achieved by complying with the following condition:

$$|\theta(\omega)|^2 + |\theta(\pi - \omega)|^2 = 1 \tag{12}$$

$$1 - \frac{a_1}{a_2} \leq \beta \leq \frac{a_3}{a_4} \tag{13}$$

Here β and ϵ are non-negative constants. With these constraints, FAWT is attuned to the following values of parameters: $a_1 = 3$, $a_2 = 4$, $a_3 = 1$, $a_4 = 2$, and $J = 15$ for the decomposition of EEG signals.

2.2.3. Properties of FAWT

This method has been widely explored in the literature due to its exclusive advantages over the other existing techniques. It owns desirable characteristics like flexible time-frequency covering by fractional scaling and shifting parameters, tunable oscillatory bases, and improved shift invariance. It is a robust rational-dilation transform which provides the flexibility to modify the parameters [42]. As mentioned above, FAWT gives Hilbert transform pairs of the wavelet bases owing to the above way of dissolution of positive and negative frequencies. It favors the definite extraction of impulse intervals and allows random setting of wavelet filters. Diverse oscillatory fault impulses can be tested with FAWT, owing to its oscillation-tunable bases. Also, changing the parameter β along with selected translation factors and scaling can finely adjust the oscillation of the FAWT bases.

2.3. Feature extraction and normalization

Flexible analytic wavelet transform decomposes the EEG signals within band-limited SBs. The attributes of the resulting SBs can be evaluated using various statistical features that contain the inter-class discrimination information for the detection of both classes of MI tasks. Here, feature selection is performed using statistical hypothesis testing. It gives an idea about the discriminatory capacity of the selected features among various classes. In the present work, a non-parametric analysis of variance, namely KW test is implemented [44]. 95% confidence level in MATLAB's Statistics Toolbox indicates that a difference is considered statistically significant if $p < \alpha(= 0.05)$.

The temporal moment is examined as a feature for the classification of MI tasks based on EEG signals. Only the third, fourth and fifth moments are taken into consideration for the assessment purpose. The temporal moment basically is a statistical analysis suggested in [45], for controlling a prosthetic arm. For the odd moment condition, the absolute value was considered to minimize the within-class separation. This work uses the third, fourth, and fifth temporal moments i.e TM3, TM4, and TM5. The following equations are used to calculate the features as:

$$TM3 = \left|\frac{1}{M}\sum_{j=1}^{M} x_j^3\right| \tag{14}$$

$$TM4 = \frac{1}{M}\sum_{j=1}^{M} x_j^4 \tag{15}$$

$$TM5 = \left|\frac{1}{M}\sum_{j=1}^{M} x_j^5\right| \tag{16}$$

where x and M signify sub-band and number of samples in sub-band, respectively. Feature normalization is used in this work to restrain the partial behavior of the classifier inclined towards a specific group of attributes [46].

2.4. Classification

The k-nearest neighbor (kNN) algorithm is an elementary machine learning technique. Here, a task or an item is classified by a majority vote of its neighbors followed by nomination to the class frequent amid its k nearest neighbors. It has been extensively used in pattern recognition due to several advantages, such as good generalization and easy implementation [47]. However, the high dimensionality of EEG usually hinders the performance of kNN. It is not optimum due to inadequate prototypes in a high dimensional feature space [48]. The complexity of such feature spaces increments exponentially with the number of features [49]. In such a situation, a technique that can exploit the benefits of kNN classifier without being adversely affected by the sparsity of high-dimensional data would be highly preferred and the well-known ensemble learning technique effectively takes advantages of high dimensionality [50].

Ensemble classifier builds *weak* or base classifiers by merging their results to yield an outcome[51]. Hence, it builds a strong classifier by exploiting the strength of each of them, eventually improving the overall classification performance [51,52]. kNN is stable to the change of the training datasets while sensitive to the variation of the feature sets [48]. As kNN is perceptive to input choices, ensembles method based random subspaces is competent to enhance the performance of single kNN classifiers. Random subspace is one of the most frequently used ensemble methods. It develops individual classifiers using randomly selected feature subspaces. Then finally, the results of each independent classifier are merged together using uniform majority voting to yield the final outcome [53]. The process is depicted in Fig. 4.

In the case of kNN classifier, when a test sample is selected as a prototype, only the chosen features are inputted to the distance. But in subspace kNN, it is the projection of all the points to the chosen subspace and the k adjacent neighbors are estimated using the distances. A new set of k-nearest neighbors are calculated whenever a random subspace is chosen. Majority vote on the class membership of the test sample is done by assembling k adjoining neighbors in each chosen subspace. The same training sample may reoccur in this ensemble if it found to be amidst the k adjacent neighbors in multiple elected subspace. Mathematical steps can be found in [50].

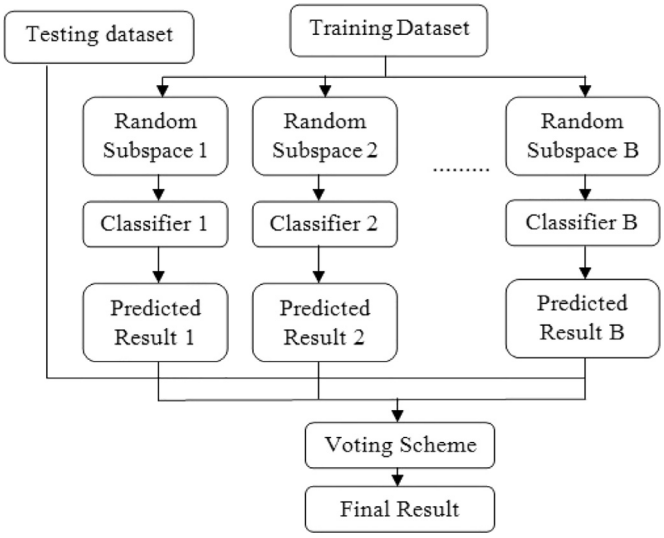

Fig. 4. Random subspace classification algorithm.

3. Results

3.1. Kruskal-Wallis statistical test

FAWT is employed for the decomposition of RH and RF MI tasks based EEG signals. Signals of both MI activites are broken down into band-limited SBs. These are then accessed by using subsequent empirically selected FAWT parameters: $a_1 = 3$, $a_2 = 4$, $a_3 = 1$, and $a_4 = 2$. Upon trial and error, it was found that these values of parameters yield maximum classification accuracy. Fifteenth level decomposition is chosen to analyze MI based EEG signals. Consequently, the value of parameters β=0.8$\left(\frac{a_3}{a_4}\right)$, d, Q, R are 0.4, 0.75, 4 and 2, respectively. The time domain measures of the resulting SBs namely temporal moment (TM3, TM4, and TM5) are examined as features. Then, feature normalization technique is tested on the derived features to abstain from their domineering behavior. The statistical significance of normalized features is estimated using probabilistic (p)-value calculated using the KW test. The p values of extracted features TM3, TM4 and TM5 is demonstrated in Tables 1–3 respectively. These tables show statistically significant (< 0.05) p-values of extracted feature. This signifies the discriminatory potential of the chosen set of features. Tables 1–3 clearly demonstrate the variations in the electrical activity of the brain corresponding to both MI tasks. The SB wise feature set is composed of all channels. Three features are derived for ten channels, thus in total 30 features are selected for each class of SBs. The dimensions of SB wise feature sets used for RH and RF EEG signal classification is 200 $\times$ 30 and 250 $\times$ 30, respectively, where rows represent the number of observations of respective classes and columns serves as the features.

3.2. Performance of various classifiers

There cannot be any generalized best machine learning model because a group of presumptions or a hypothesis that work for one domain may not be suited to another domain. Consequently, a wise approach would be to test numerous different models in order to achieve an improved result. This way the algorithm works realistically. Thus, a multiple classifier analysis is adopted in the present work to find out the best classifier for identification of two class MI tasks. Initially, various classifiers were tested on the extracted features. Implementation of SVM, ensemble methods, discriminant analysis (DA), k-nearest neighbors (kNN), and decision trees (DT) along with their variants is carried out. Table 4 shows the results obtained using the above-mentioned classifiers. For kNN, k is varied from 1, 2, 3,..., 100, and the accuracy of each class is found out. kNN variants such as fine, medium, cubic, etc. are employed. The best results are listed in Table 4. For DA, evaluation is done using linear and quadratic discriminant functions. As for SVM, linear and quadratic functions are used for calculation. Variants of DT are further tested on the selected features. The results are illustrated in Table 4. It demonstrates that subspace kNN arises as the best classifier exceeding others in terms of classification accuracy. It authenticates that subspace kNN is an assuring and promising choice for

Table 1
Probabilistic values for TM3 feature for SBs of different channel EEG signals.

	SB1	SB2	SB3	SB4	SB5	SB6	SB7	SB8
CH1	2.21×10^{-20}	1.62×10^{-13}	1.87×10^{-74}	6.38×10^{-72}	2.14×10^{-76}	2.78×10^{-70}	3.25×10^{-75}	6.72×10^{-46}
CH2	0.0566	2.15×10^{-55}	3.08×10^{-38}	9.84×10^{-08}	1.61×10^{-73}	2.75×10^{-29}	1.71×10^{-72}	1.25×10^{-35}
CH3	7.72×10^{-25}	6.31×10^{-49}	1.49×10^{-66}	4.04×10^{-65}	4.43×10^{-74}	2.16×10^{-72}	3.55×10^{-68}	5.98×10^{-35}
CH4	6.64×10^{-18}	1.52×10^{-66}	1.93×10^{-62}	2.69×10^{-70}	7.07×10^{-52}	1.77×10^{-56}	4.01×10^{-68}	6.02×10^{-29}
CH5	2.67×10^{-17}	2.33×10^{-64}	1.27×10^{-56}	3.78×10^{-70}	2.88×10^{-76}	1.09×10^{-68}	7.66×10^{-71}	9.71×10^{-44}
CH6	0.017	3.57×10^{-31}	6.70×10^{-37}	5.27×10^{-52}	6.06×10^{-67}	6.03×10^{-55}	3.48×10^{-52}	5.13×10^{-33}
CH7	1.24×10^{-14}	1.74×10^{-64}	6.94×10^{-66}	2.11×10^{-72}	1.08×10^{-66}	8.52×10^{-74}	4.83×10^{-76}	4.09×10^{-31}
CH8	2.78×10^{-07}	1.18×10^{-29}	7.05×10^{-27}	1.15×10^{-43}	4.83×10^{-10}	3.16×10^{-15}	1.67×10^{-25}	1.57×10^{-08}
CH9	2.41×10^{-09}	1.96×10^{-26}	4.93×10^{-43}	2.47×10^{-52}	3.95×10^{-45}	6.16×10^{-63}	2.01×10^{-66}	9.79×10^{-39}
CH10	4.93×10^{-12}	5.71×10^{-49}	1.26×10^{-61}	2.23×10^{-72}	5.13×10^{-75}	2.72×10^{-66}	8.82×10^{-77}	3.73×10^{-35}

Table 2
Probabilistic values for TM4 feature for SBs of different channel EEG signals.

	SB1	SB2	SB3	SB4	SB5	SB6	SB7	SB8
CH1	1.27×10^{-66}	4.92×10^{-69}	4.23×10^{-75}	1.75×10^{-77}	4.09×10^{-79}	2.63×10^{-79}	2.30×10^{-68}	4.33×10^{-43}
CH2	0.3388	4.70×10^{-53}	2.88×10^{-65}	4.31×10^{-71}	1.07×10^{-67}	4.08×10^{-65}	2.24×10^{-58}	1.49×10^{-43}
CH3	9.65×10^{-66}	2.01×10^{-71}	3.04×10^{-75}	5.56×10^{-77}	9.72×10^{-78}	1.16×10^{-76}	1.05×10^{-66}	2.60×10^{-44}
CH4	9.52×10^{-49}	4.86×10^{-68}	6.93×10^{71}	2.67×10^{-72}	4.76×10^{-73}	2.01×10^{-69}	2.99×10^{-56}	1.58×10^{-36}
CH5	1.86×10^{-38}	1.24×10^{-61}	6.70×10^{-70}	8.06×10^{-74}	1.25×10^{-75}	1.01×10^{-72}	1.54×10^{-61}	4.33×10^{-43}
CH6	1.77×10^{-10}	3.73×10^{-18}	1.46×10^{-34}	1.34×10^{-53}	1.53×10^{-68}	2.46×10^{-66}	1.33×10^{-64}	8.51×10^{-35}
CH7	1.73×10^{-55}	9.62×10^{-68}	5.46×10^{-72}	2.71×10^{-75}	3.31×10^{-77}	6.70×10^{-78}	3.89×10^{-77}	1.71×10^{-39}
CH8	1.76×10^{-14}	5.51×10^{-37}	6.35×10^{-37}	2.82×10^{-38}	5.29×10^{-39}	1.35×10^{-29}	1.77×10^{-13}	8.95×10^{-13}
CH9	1.16×10^{-06}	6.66×10^{-14}	2.48×10^{-29}	3.19×10^{-48}	4.96×10^{-56}	1.16×10^{-63}	6.31×10^{-68}	3.88×10^{-39}
CH10	6.69×10^{-44}	2.44×10^{-61}	2.94×10^{-63}	7.05×10^{-72}	9.37×10^{-75}	7.37×10^{-76}	1.52×10^{-75}	5.21×10^{-40}

Table 3
Probabilistic values for TM5 feature for SBs of different channel EEG signals.

	SB1	SB2	SB3	SB4	SB5	SB6	SB7	SB8
CH1	6.24×10^{-41}	9.64×10^{-63}	2.31×10^{-65}	1.24×10^{-77}	5.31×10^{-77}	3.38×10^{-76}	7.48×10^{-70}	2.75×10^{-39}
CH2	0.0009	6.49×10^{-31}	3.23×10^{-33}	3.62×10^{-60}	2.87×10^{-57}	7.28×10^{-53}	1.07×10^{-55}	6.24×10^{-36}
CH3	3.97×10^{-39}	1.26×10^{-59}	2.36×10^{-65}	1.27×10^{-71}	2.09×10^{-72}	1.16×10^{-71}	4.27×10^{-68}	7.01×10^{-34}
CH4	2.28×10^{-17}	5.95×10^{-43}	1.43×10^{-54}	3.17×10^{-65}	8.13×10^{-65}	1.11×10^{-61}	3.54×10^{-57}	5.58×10^{-31}
CH5	9.78×10^{-12}	1.81×10^{-43}	6.36×10^{-54}	2.30×10^{-68}	1.37×10^{-66}	2.15×10^{-66}	4.47×10^{-64}	3.46×10^{-39}
CH6	0.0186	2.30×10^{-14}	3.39×10^{-23}	6.39×10^{-64}	1.47×10^{-61}	1.48×10^{-65}	1.13×10^{-59}	2.84×10^{-32}
CH7	9.80×10^{-24}	7.61×10^{-46}	1.07×10^{-53}	2.24×10^{-71}	4.28×10^{-74}	4.63×10^{-74}	2.03×10^{-74}	1.36×10^{-32}
CH8	1.04×10^{-10}	4.95×10^{-28}	6.34×10^{-28}	4.88×10^{-28}	5.78×10^{-33}	7.11×10^{-26}	5.58×10^{-27}	1.51×10^{-07}
CH9	5.72×10^{-05}	0.0273	7.80×10^{-08}	2.51×10^{-46}	1.92×10^{-47}	1.70×10^{-61}	2.54×10^{-63}	4.31×10^{-37}
CH10	1.14×10^{-17}	3.14×10^{-34}	5.92×10^{-39}	3.90×10^{-69}	2.26×10^{-70}	4.57×10^{-72}	7.81×10^{-73}	6.79×10^{-36}

Table 4
Performance of various classifiers for the proposed method.

Classifier	Classifier variant	Sub-band wise classification accuracy							
		SB1	SB2	SB3	SB4	SB5	SB6	SB7	SB8
SVM	Linear SVM	83.1	88.9	84.7	94	87.3	78	80.7	88.7
	Quadratic SVM	50.9	84	79.6	95.1	94.2	92	88.4	54.9
	Boosted trees	55.6	55.6	55.6	55.6	55.6	55.6	55.6	88.2
Ensemble	Bagged trees	97.6	97.1	97.8	97.8	98.2	97.1	97.8	93.6
Learning	Subspace discriminant	57.1	55.1	54.4	54.7	90.4	74.7	78.9	88.9
	Subspace kNN	86.9	97.56	96.7	**99.33**	98	97.78	97.56	94
	RUSboost	95.1	94.7	91.6	80.7	88.7	91.1	85.1	93.1
	Fine kNN	95.1	96.7	96	96	96.4	96.4	96	96.4
	Medium kNN	94.9	94.9	96	95.8	96.4	95.6	95.8	95.3
	Coarse kNN	85.1	87.1	87.1	86.7	87.6	86.2	86.7	87.1
NN	Cosine kNN	92.2	92.7	92.7	92.2	93.1	92.4	92.7	92.9
	Cubic kNN	94.2	94.7	96	95.6	95.8	95.8	96.2	95.3
	Weighted kNN	95.8	95.8	96.7	96.9	96	96.2	96.9	96
Decision	Complex tree	96.9	98.2	97.6	96.9	97.1	97.8	97.6	96.4
trees	Medium tree	96.9	98.2	97.6	96.9	97.1	97.8	97.6	96.4
	Simple tree	96.9	97.8	97.6	96.9	97.6	97.8	97.1	96.4
Discriminant	Linear discriminant	78.9	79.6	79.8	78.2	80	78.4	78.7	79.3
Analysis	Quadratic discriminant	93.8	93.3	93.3	93.6	93.6	93.6	93.3	93.8

Table 5
SB wise classification performance parameters using subspace kNN classifier.

	ACC(%)	SEN(%)	SPE(%)	F1-Score	Kappa	Error (%)
SB1	86.9	86	88.8	0.86	0.748	12.44
SB2	97.56	97.5	97.6	0.972	0.9503	2.44
SB3	96.67	95	98	0.962	0.9323	3.33
SB4	99.33	99	99.6	0.9925	0.9865	0.67
SB5	98	97	98.8	0.9746	0.9549	2.22
SB6	97.78	96	99.2	0.9674	0.9415	2.89
SB7	97.56	98	97.2	0.9727	0.9506	2.44
SB8	94	92	95.6	0.9316	0.8782	6

classification of MI tasks based on EEG signals. The computation of classification accuracy using multiple classifiers is done using the 10-fold cross-validation method. 10-fold cross-validation technique evaluates the models by dividing the original feature vector set into ten subsets, where one of them is considered as the testing set and the remaining nine are the training set for the classifier. The ten subsets are mutually exclusive and the process is iterated ten times. This method overcomes the issue of underfitting and significantly decreases the variance of the data. The classification effectiveness of the recommended method is appraised in terms of error, accuracy (ACC), F1-score, kappa value, specificity (SPE) and sensitivity (SEN) parameters. The overall performance is the average of the accuracy values from all the ten trials. Table 5 shows SB wise performance parameters obtained using the ensemble method based subspace kNN classifier. The best results of parameters are obtained for fourth SB as ACC 99.33%, SEN 99%, SPE 99.6%, error 0.67%, F1-Score 0.9925 and kappa value as 0.9865. Other SBs have also given significant results using subspace KNN classifier. In is noticed from the Table 4 the subspace KNN classifier with FAWT based features provides better classification accuracy. All the simulations are done using MATLAB 2017a on a computer with Intel(R) Core(TM) i3-5010U, 2.10 GHz CPU, 4 GB of RAM.

3.3. Performance comparison

To further appraise the efficiency, Table 6 shows the report on comparative performance analysis of the proposed method with previously existing same base dataset methods. The comparison is done on the basis of the classification accuracy achieved. It shows methods such as OAS together with NB classifier, CC technique with LS-SVM as classifier has already been proposed, achieving a classification accuracy of 96.36% and 81.1% respectively. Similarly, a few other methods are also given employing TQWT, Z-Score, and multiscale principal component analysis (MSPCA) with HOS and RCSP with aggregation. The classification accuracy obtained using these prominent methods is indicated in Table 6. The highest accuracy that was achieved before was 97.56%. It clearly indicates that the proposed approach has accomplished the highest classification accuracy of 99.33%. It has outperformed various other good combinations of feature extraction methods and classifiers. Table 6 approves the combination of FAWT with ensemble-based subspace KNN for the mentioned purpose. The obtained results validate the efficacy and robustness of the proposed method towards distinction of different MI tasks in a BCI system. It can find various applications in different fields.

4. Discussion

As mentioned previously, the purpose of the present study is to achieve better classification accuracy for the distinction of RH

Table 6
Performance comparison of proposed method with recent reported same data set methods.

Author and Year	Methods	Classifier	Accuracy(%)
Proposed Approach	FAWT	Subspace kNN	**99.3**
Li et al. [16]	CC	LS-SVM	95.72
Zhang et al. [8]	Z-score	LDA	81.1
Siuly et al. [28]	CC	LR	91.79
Ince et al. [25]	CS	SVM	96
Siuly et al. [18]	OA	NB	96.36
Kevric et al. [19]	MSPCA, WPD, HOS	k-NN	92.8
Li et al. [22]	OA	LS-SVM	96.62
Verma et al. [30]	DWT	LS-SVM	96.1
Siuly et al. [17]	CT	LS-SVM	88.32
Taran et al. [27]	TQWT	LS-SVM	96.89
Lu et al. [14]	R-CSP with aggregation	R-CSP	83.9
Taran et al. [29]	EMD	LS-SVM	97.56

and RF MI tasks based on EEG signals. Due to the non-stationary nature of EEG signals, the present work proposes FAWT based decomposition of different MI tasks EEG signals into band-limited SBs. The values [30] of the FAWT parameters and the level of decomposition are chosen on an experimental basis. It is further followed by feature extraction and selection process. The assessment is carried out using the KW test for determining the statistical significance of extracted features. KW is essentially a nonparametric evaluation of variance, independent of any requirement of an assumption of normally distributed data. The results allow to select the features with good discriminatory power. Third, fourth and fifth temporal moments are considered as features. These particular features are preferred due to their lower p-values and satisfactory range deviation as shown in Tables 1–3 for both classes of MI tasks based EEG signals. Eventually, the classification performance of extracted FAWT based features is evaluated using multiple classifiers in order to achieve the best classification accuracy. Several multiple classification models are implemented for the proposed FAWT-based features where excellent results are obtained using subspace kNN classifier. Thus, the multi-classifier approach explores the utility and robustness of the ensemble method based on subspace kNN. The 10-fold cross validation method is used to achieve consistent and reliable performance and extensively to refrain from over-fitting of the model.

Tables 4 and 5 collectively prove the effectiveness of our proposed method, in turn making it a reliable and accurate solution for the concerned issue. Table 4 signifies the effectiveness of employing multiple classifiers in our approach. This type of approach towards the classification of MI tasks in a BCI system using FAWT has been utilized for the first time in the literature. It shows the classic classifiers and their variants that were implemented in this multiple classifier analysis. Variants of SVM namely linear and quadratic SVM are used for testing on selected features where quadratic SVM has outperformed linear SVM for most of the sub-bands, achieving the highest accuracy of 95.1% for fourth SB. Similarly, various variants of kNN classifier have been tested. The results obtained using these classifiers are also satisfactory, most of them being above 95%. Best performance that could be achieved is using weighted kNN classifier for third SB with an accuracy of 96.7%. Further, three variants of DT were tested that also gave impressive results, a large proportion being around 97% accuracy. Here the performance of all three variants namely complex, medium and simple tree is almost identical. The last rows in Table 4 illustrate the performance of LDA and QDA in distinguishing the MI tasks. Here, it can be directly concluded that QDA has outperformed LDA. Multiple classifier approaches using various base classifier and their variants helped to explore the robustness and utility of ensemble learning classifier and finally, subspace KNN is established as the best classifier for our purpose. From Table 5, the sensitivity of 0.990 for fourth SB indicates that 99 of 100 RH MI tasks are correctly classified as RH. Similarly, the specificity value of 0.9960 indicates the proportion of total RF MI tasks that are accurately recognized as RF tasks. Thus, the error rate or misclassification is minimal. The proposed approach has also obtained a high value of F1-Score as 0.9925 which is very close to its highest value one. This signifies the accurate performance of the proposed work. Also, a kappa value of 0.9865 indicates the effectiveness of subspace KNN classifier in detecting the two MI tasks. Thus, the performance of the classifier is also evaluated and in comparison to other classifiers, it has proven to be the best for the mentioned purpose. On the whole, the classification accuracy of 99.33% shows how effectively the presented method is able to recognize the binary classes of MI tasks. Such high classification accuracy indicates the reliability and robustness of the method towards the identification of different MI tasks in a BCI system. Table 6 concludes that it proves to be accurate, veracious and powerful on comparison with previously given methods. Therefore, it can be employed in various applications such as wheelchair controlling for disabled, robotic arm, mouse controlling, etc. It can be used to make a huge influence on the lives of its beneficiaries.

5. Conclusion

The proposed work explores the utility of FAWT based features for the classification of RH and RF MI tasks based on EEG signals. FAWT is employed to decompose EEG signals into SBs. Later, time domain feature namely temporal moment (TM3, TM4, and TM5) are used for examining the characteristics of the resulting SBs. Feature normalization is adapted to control the biased nature of extracted features. The discriminatory ability of these three features is computed using the KW test. All three of them have displayed smaller p values. Thus they have the good discriminatory ability. Further, multiple classifiers are engaged to test these statistically significant features. SVM, kNN, discriminant analysis, decision trees are used for obtaining a robust solution but ensemble method based subspace kNN outperforms others. Performance parameters are estimated for each SB. Fourth SB provides the best results with a classification accuracy of 99.3%, the sensitivity of 99%, specificity as 99.6%, F1-score of 0.9925 and kappa value as 0.9865. Also, the proposed method is best when compared to previously existing methods worked upon the same dataset. Thus, this approach of using FAWT as signal decomposition method and multiple classifier analysis is the best step towards the classification of different MI tasks. The suggested method highlights the effectiveness of using multiple classifiers for classification. The results give hope for advancement in BCI applications utilizing the distinction of MI tasks such as wheelchair controlling. It could leave a huge imprint on the lives of many. In the future, an expert

algorithm can be optimized to obtain the FAWT parameter values for the analysis of EEG signals.

Declaration of Competing Interest

None.

Supplementary material

Supplementary material associated with this article can be found, in the online version, at 10.1016/j.cmpb.2020.105325.

References

[1] C.A.S. Filho, R. Attux, G. Castellano, Can graph metrics be used for EEG-BCIs based on hand motor imagery? Biomed. Signal Process. Control 40 (2018) 359–365.
[2] H. Yuan, B. He, Brain-computer interfaces using sensorimotor rhythms: current state and future perspectives, IEEE Trans. Biomed. Eng. 61 (5) (2014) 1425–1435.
[3] Y. Li, P.P. Wen, et al., Modified CC-LR algorithm with three diverse feature sets for motor imagery tasks classification in EEG based brain-computer interface, Comput. Methods Programs Biomed. 113 (3) (2014) 767–780.
[4] L. Kauhanen, T. Nykopp, J. Lehtonen, P. Jylanki, J. Heikkonen, P. Rantanen, H. Alaranta, M. Sams, EEG and MEG brain-computer interface for tetraplegic patients, IEEE Trans. Neural Syst. Rehabil. Eng. 14 (2) (2006) 190–193.
[5] A. Ahangi, M. Karamnejad, N. Mohammadi, R. Ebrahimpour, N. Bagheri, Multiple classifier system for EEG signal classification with application to brain–computer interfaces, Neural Comput. Appl. 23 (5) (2013) 1319–1327.
[6] A.R. Hassan, A. Subasi, Automatic identification of epileptic seizures from EEG signals using linear programming boosting, Comput. Methods Programs Biomed. 136 (2016) 65–77.
[7] R. Zhang, P. Xu, L. Guo, Y. Zhang, P. Li, D. Yao, Z-Score linear discriminant analysis for EEG based brain-computer interfaces, PLoS ONE 8 (9) (2013) e74433.
[8] Y. Zhang, C.S. Nam, G. Zhou, J. Jin, X. Wang, A. Cichocki, Temporally constrained sparse group spatial patterns for motor imagery BCI, IEEE Trans. Cybern. (99) (2018) 1–11.
[9] S. Saha, K.I. Ahmed, R. Mostafa, Wavelet coherence based channel selection for classifying single trial motor imagery, in: Electrical and Computer Engineering (ICECE), 2016 9th International Conference on, IEEE, 2016, pp. 467–470.
[10] L. Duan, Z. Hongxin, M.S. Khan, M. Fang, Recognition of motor imagery tasks for BCI using CSP and chaotic PSO twin SVM, J. China Univ. PostsTelecommun. 24 (3) (2017) 83–90.
[11] S. Kumar, A. Sharma, K. Mamun, T. Tsunoda, A deep learning approach for motor imagery EEG signal classification, in: Computer Science and Engineering (APWC on CSE), 2016 3rd Asia-Pacific World Congress on, IEEE, 2016, pp. 34–39.
[12] N. Robinson, A.P. Vinod, C. Guan, K.K. Ang, T.K. Peng, A wavelet CSP method to classify hand movement directions in EEG based BCI system, in: Information, Communications and Signal Processing (ICICS) 2011 8th International Conference on, IEEE, 2011, pp. 1–5.
[13] H. Lu, H.-L. Eng, C. Guan, K.N. Plataniotis, A.N. Venetsanopoulos, Regularized common spatial pattern with aggregation for EEG classification in small-sample setting, IEEE Trans. Biomed. Eng. 57 (12) (2010) 2936–2946.
[14] H.-I. Suk, S.W. Lee, A novel bayesian framework for discriminative feature extraction in brain-computer interfaces, IEEE Trans. Pattern Anal. Mach. Intell. 35 (2) (2013) 286–299.
[15] S. Siuly, Y. Li, Improving the separability of motor imagery EEG signals using a cross correlation-based least square support vector machine for brain-computer interface, IEEE Trans. Neural Syst. Rehabil. Eng. 20 (4) (2012) 526–538.
[16] Y. Li, P.P. Wen, et al., Clustering technique-based least square support vector machine for EEG signal classification, Comput. Methods Programs Biomed. 104 (3) (2011) 358–372.
[17] H. Wang, Y. Zhang, et al., Detection of motor imagery EEG signals employing Naive Bayes based learning process, Measurement 86 (2016) 148–158.
[18] J. Kevric, A. Subasi, Comparison of signal decomposition methods in classification of EEG signals for motor-imagery BCI system, Biomed. Signal Process. Control 31 (2017) 398–406.
[19] S.-M. Zhou, J.Q. Gan, F. Sepulveda, Classifying mental tasks based on features of higher-order statistics from EEG signals in brain-computer interface, Inf. Sci. 178 (6) (2008) 1629–1640.
[20] Y. Fang, M. Chen, X. Zheng, Extracting features from phase space of EEG signals in brain- computer interfaces, Neurocomputing 151 (2015) 1477–1485.
[21] H. Mirvaziri, Z.S. Mobarakeh, Improvement of EEG-based motor imagery classification using ring topology-based particle swarm optimization, Biomed. Signal Process. Control 32 (2017) 69–75.
[22] D.H. Krishna, I. Pasha, T.S. Savithri, Classification of EEG motor imagery multi class signals based on cross correlation, Procedia Comput. Sci. 85 (2016) 490–495.
[23] T. Nguyen, A. Khosravi, D. Creighton, S. Nahavandi, Fuzzy system with tabu search learning for classification of motor imagery data, Biomed. Signal Process. Control 20 (2015) 61–70.
[24] N.F. Ince, F. Goksu, A.H. Tewfik, S. Arica, Adapting subject specific motor imagery EEG patterns in space-time-frequency for a brain computer interface, Biomed. Signal Process. Control 4 (3) (2009) 236–246.
[25] M.E. Alam, B. Samanta, Empirical mode decomposition of EEG signals for brain computer interface, in: Southeast Con, 2017, IEEE, 2017, pp. 1–6.
[26] S. Taran, V. Bajaj, Motor imagery tasks-based EEG signals classification using tunable-q wavelet transform, Neural Comput. Appl. (2018) 1–8.
[27] L.F. Nicolas-Alonso, R. Corralejo, J. Gomez-Pilar, D. Alvarez, R. Hornero, Ensemble learning for classification of motor imagery tasks in multiclass brain computer interfaces, in: Computer Science and Electronic Engineering Conference (CEEC), 2014 6th, IEEE, 2014, pp. 79–84.
[28] M.Z. Baig, N. Aslam, H.P. Shum, L. Zhang, Differential evolution algorithm as a tool for optimal feature subset selection in motor imagery EEG, Expert Systems with Applications 90 (2017) 184–195. 24
[29] S. Taran, V. Bajaj, D. Sharma, S. Siuly, A. Sengur, Features based on analytic IMF for classifying motor imagery EEG signals in BCI applications, Measurement 116 (2018) 68–76.
[30] N.K. Verma, L.V.S. Rao, S.K. Sharma, Motor imagery EEG signal classification on DWT and crosscorrelated signal features, in: Industrial and Information Systems (ICIIS), 2014 9th International Conference on, IEEE, 2014, pp. 1–6.
[31] Y. Yang, S. Chevallier, J. Wiart, I. Bloch, Subject-specific time-frequency selection for multi-class motor imagery-based BCIs using few Laplacian EEG channels, Biomed. Signal Process. Control 38 (2017) 302–311.
[32] P. Gaur, R.B. Pachori, H. Wang, G. Prasad, A multi-class EEG-based BCI classification using multivariate empirical mode decomposition based filtering and Riemannian geometry, Expert Syst. Appl. 95 (2018) 201–211.
[33] E. Hortal, D. Planelles, A. Costa, E. Ianez, A. Ubeda, J.M. Azorin, E. Fernandez, SVM-based brain-machine interface for controlling a robot arm through four mental tasks, Neurocomputing 151 (2015) 116–121.
[34] M. Kumar, R.B. Pachori, U.R. Acharya, An efficient automated technique for CAD diagnosis using flexible analytic wavelet transform and entropy features extracted from HRV signals, Expert Syst. Appl. 63 (2016) 165–172.
[35] D. Li, J. Zhou, J. Zhao, X. Liu, J wave autodetection using analytic time frequency flexible wavelet transformation applied on ECG signals, Math. Prob. Eng. (2018).
[36] C. Zhang, B. Li, B. Chen, H. Cao, Y. Zi, Z. He, Weak fault signature extraction of rotating machinery using flexible analytic wavelet transform, Mech. Syst. Signal Process. 64 (2015) 162–187.
[37] V. Gupta, T. Priya, A.K. Yadav, R.B. Pachori, U.R. Acharya, Automated detection of focal EEG signals using features extracted from flexible analytic wavelet transform, Pattern Recognit. Lett. 94 (2017) 180–188.
[38] M. Sharma, R.B. Pachori, U.R. Acharya, A new approach to characterize epileptic seizures using analytic time-frequency flexible wavelet transform and fractal dimension, Pattern Recognit. Lett. 94 (2017) 172–179.
[39] M. Kumar, R.B. Pachori, U.R. Acharya, Characterization of coronary artery disease using flexible analytic wavelet transform applied on ECG signals, Biomed. Signal Process. Control 31 (2017) 301–308.
[40] V. Bajaj, S. Taran, A. Sengur, Emotion classification using flexible analytic wavelet transform for electroencephalogram signals, Health Inf. Sci. Syst. 6 (1) (2018) 12.
[41] B. Blankertz, K.-R. Muller, D.J. Krusienski, G. Schalk, J.R. Wolpaw, A. Schlogl, G. Pfurtscheller, J.R. Millan, M. Schroder, N. Birbaumer, The BCI competition III: validating alternative approaches to actual BCI problems, IEEE Trans. Neural Syst. Rehabil. Eng. 14 (2) (2006) 153–159.
[42] I. Bayram, An analytic wavelet transform with a flexible time-frequency covering, IEEE Trans. Signal Process. 61 (5) (2013) 1131–1142.
[43] U.R. Acharya, H. Fujita, M. Adam, O.S. Lih, V.K. Sudarshan, T.J. Hong, J.E. Koh, Y. Hagiwara, C.K. Chua, C.K. Poo, et al., Automated characterization and classification of coronary artery disease and myocardial infarction by decomposition of ECG signals: a comparative study, Inf. Sci. 377 (2017) 17–29.
[44] W.H. Kruskal, W. A. Wallis, Use of ranks in one-criterion variance analysis, J. Am. Stat. Assoc. 47 (260) (1952) 583–621.
[45] G.N. Saridis, T.P. Gootee, EMG pattern analysis and classification for a prosthetic arm, IEEE Trans. Biomed. Eng. (6) (1982) 403–412.
[46] M. Shanker, M.Y. Hu, M.S. Hung, Effect of data standardization on neural network training, Omega 24 (4) (1996) 385–397.
[47] T. Cover, P. Hart, Nearest neighbor pattern classification, IEEE Trans. Inf. Theory 13 (1) (1967) 21–27.
[48] K. Fukunaga, D.M. Hummels, Bias of nearest neighbor error estimates, IEEE Trans. Pattern Anal. Mach. Intell. (1) (1987) 103–112.
[49] P. Mewada, J. Patil, Performance analysis of k-NN on high dimensional datasets, Int. J. Comput. Appl. 16 (2) (2011) 1–5.
[50] T.K. Ho, Nearest neighbors in random subspaces, in: Joint IAPR International Workshops on Statistical Techniques in Pattern Recognition (SPR) and Structural and Syntactic Pattern Recognition (SSPR), Springer, 1998, pp. 640–648.
[51] S. Sun, C. Zhang, D. Zhang, An experimental evaluation of ensemble methods for EEG signal classification, Pattern Recognit. Lett. 28 (15) (2007) 2157–2163.
[52] Y. Chen, M.L. Wong, Optimizing stacking ensemble by an ant colony optimization approach, in: Proceedings of the 13th Annual Conference Companion on Genetic and Evolutionary Computation, ACM, 2011, pp. 7–8.
[53] T.K. Ho, Random decision forests, in: Document Analysis and Recognition, 1995. Proceedings of the Third International Conference on, vol. 1, IEEE, 1995, pp. 278–282.